npj climate and atmospheric science

www.nature.com/npjclimatsci

EDITORIAL OPEN

Check for updates

# Occurrence and hotspots of multivariate and temporally compounding events in China from 1961 to 2020

Due to the greater negative impacts on humans and ecosystems, compound events (CEs) have received increasing attention in China over recent decades. Previous studies mainly considered combinations of frequent hazards (e.g., extreme hot and dry events or heatwaves and extreme precipitation), potentially leading to an inadequate understanding of CEs hotspots, as the occurrence of CEs varies considerably with the diverse hazard types and their temporal sequence (multivariate compound events (MCEs) and temporally compounding events (TCEs)). Here, using daily meteorological observations from 1961 to 2020, we identify 44 CEs types considering the temporal sequences of various hazards from that period and explore their occurrence patterns in China. The results show that 12 CEs types related to extreme hot or dry events widely and frequently (return period < 1 year) occur in China, particularly compound extreme hot-dry-high fire risk events (return period of 0.2–0.4 yrs). Regarding the temporal sequences, MCEs and TCEs have similar spatial distributions, but the magnitudes of MCEs are approximately 1.1 to 2.6 times those of TCEs. This difference is obvious in CEs formed by multiple hazards (>2). By considering occurrence patterns (return period and magnitude), temporal trends, and correlations between different hazards, we determine that the southern humid regions of China are prone to CEs. These results provide a general reference on the national scale for identifying CEs hotspots where more climate action is needed in the future.

*npj Climate and Atmospheric Science* (2023)6:168 ;
https://doi.org/10.1038/s41612-023-00491-3

## INTRODUCTION

In eastern Australia, hundreds of wildfires occurred during the 2019–2020 fire seasons following an extreme drought, with a total burned area of more than 186,000 $km^2$ [1]. Unfortunately, the burned areas are subject to soil erosion and erosion in response to consecutive rainfall, leading to flooding and poor water quality[2,3]. Not coincidentally, during the nonfire seasons, unprecedented compound heatwave-drought events in the Sichuan-Chongqing region (SCR), Southwest China, caused several fires in the summer of 2022[4]. The above two extreme events can be termed a compound events (CEs) involving the simultaneous or successive occurrence of multiple hazards[5,6]. Although CEs are viewed as low-probability occurrences, they will become more frequent due to climate warming and have greater socioeconomic consequences[7,8]. Given the complexity and far-reaching impacts of such events, identifying the occurrence patterns and hotspots of CEs is of scientific and practical importance for climate risk adaptation[6,9,10].

Previous studies have focused on exploring the spatiotemporal patterns of various compound events, such as combined hot-drought[11,12], hot/drought-wildfire[13–15], and floods[16–18]. They provided valuable results for our understanding of CEs occurrence. For example, a global study presented a theoretical framework for analyzing the spatiotemporal patterns of the co-occurrence of two hazards across various geographic regions[19]. In the Northern Hemisphere, more than 55% of the regions showed an increase in the frequency, number of days, and severity of combined heat-drought extremes over the past decades[20]. From a sequence of occurrence perspective, two types of compound events (multivariate compound events (MCEs) and temporally compounding events (TCEs)) have been summarized and widely used to enhance the understanding of compound events[5,6]. MCEs are defined as the co-occurrence of two or more hazards in the same geographical area at the same time. Most studies have mainly focused on the occurrence patterns of MCEs formed by two hazards on national[21–23] or global scales[10,19], but little is known about the occurrence patterns and hotspots of MCEs formed by multiple (>2) hazards on a larger scale. TCEs refer to a succession of single-type or multiple types of hazards that sequentially occur in each geographical region without interruptions, leading to or amplifying impacts when compared to the impact of a single hazard[5]. For instance, high temperatures and wildfires following persistent drought[3,13] and flooding events triggered by extreme precipitation lasting several days[24–26]. Recent studies have also examined the occurrence patterns of TCEs and their spatiotemporal trends, such as temporally compound extreme heat-precipitation events (i.e., extreme precipitation events preceded by extreme heat)[27–29] and precipitation whiplash events (wet to dry or dry to wet whiplash events)[30].

China is a hotspot for climate risk due to its fast warming rate[31] of 0.16 °C per decade from 1901 to 2022, which is remarkably faster than the global average rate[32]. Recent studies have mainly explored the occurrence patterns of CEs on national or regional scales, including compound hot events[33–35], hot-drought[36–38], temporally compound hot-extreme precipitation events[27–29], and extreme precipitation-strong wind events[23]. However, focusing on only two hazards does not sufficiently define and detect all relevant conditions, which may lead to underestimation of the potential risks of CEs[39]. For example, if we only combine heatwave and drought indices to analyze CEs in Southwest China in 2022, we would ignore the impacts of wildfires on resources and underestimate the risk of compound heatwave-drought-wildfire events. However, it is unclear how many combinations of multiple (>2) hazards exist and what characteristics these CEs types would have on the national scale.

Here, we calculate six different hazard types (Supplementary Table 1) from observational data from 1961 to 2020 and form 44 CEs types (Supplementary Table 2). We employ four indices to identify the hotspots and spatiotemporal patterns of MCEs and TCEs over the past six decades, including their probabilities, return periods, magnitudes, and durations. These results can enhance our understanding of the occurrence patterns and characteristics

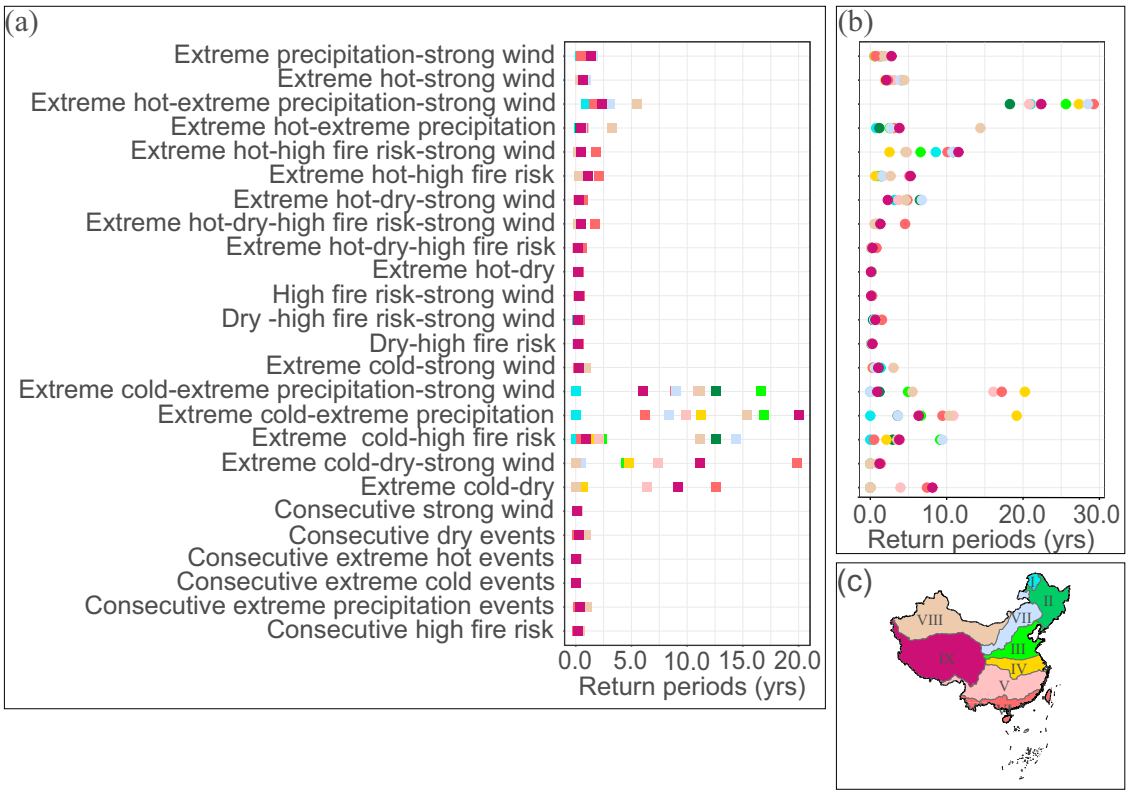


**Fig. 1 Return periods (yrd) of compound events in nine eco-geographical regions of China during 1961–2020. a, b** represents the return periods of TCEs (rectangle) and MCEs (circle) over the study period respectively; (**c**) is the spatial locations of different eco-geographical regions in China. Where (I) to (IX) are the cold temperate humid region, mid-temperate humid/subhumid region, warm temperate humid/subhumid region, northern subtropical humid region, mid-subtropical humid region, southern subtropical and tropical humid region, north semiarid region, northwest arid region, and Tibetan Plateau region (the same below).

of CEs in China and provide scientific guidance for climate risk assessment in the future.

## RESULTS

### Occurrence of MCEs and TCEs

The return periods of every CEs in different regions are presented in Fig. 1, and their hotspots can be identified. From the perspective of MCEs, MCEs of hot-dry, dry-high fire risk, high fire risk-strong wind, and hot-dry-high fire risk occur broadly in China over the past six decades and have a high frequency in all subregions (return period <1 year). Some MCEs display remarkable regional signatures. For example, the hotspots (return period <1 year) of MCEs of hot-high fire risk and hot-dry-high fire risk-strong wind are concentrated in the cold temperate humid region and northern subtropical humid region. MCEs of cold-high fire risk, cold-strong wind, and cold-dry-strong wind do not occur in the cold temperate humid region over the past six decades, and their hotspots are in the mid-subtropical humid region and southern subtropical and tropical humid region, with a return period of less than one year. The MCEs of hot-extreme precipitation-strong wind have a lower frequency throughout China from 1961 to 2020, and the return period is 18 to 29 years. The return period of other MCEs is approximately 1 to 15 years.

TCEs formed by the consecutive occurrence of the same hazard occur broadly in China from 1961 to 2020, with a shorter return period of less than 1 year. Among the TCEs formed by different hazards, the hotspots of TCEs of hot-dry, dry-high fire risk, high fire risk-strong wind, and hot-dry-high fire risk have similar spatial distributions with MCEs formed by the same hazards. These TCEs also occur broadly in China and have a higher frequency (return period <1 year). In addition, the hotspot areas of some TCEs related to strong wind (hot-strong wind, cold-strong wind, hot-dry-strong wind, and dry-high fire risk-strong wind) are significantly larger than those of corresponding MCEs formed by the same hazards, and their return periods are significantly shorter than those of MCEs in the same regions. TCEs of hot-extreme precipitation are also a major CEs type except in the northwestern arid region from 1961 to 2020, with a higher frequency (return period <1 year) in other humid/subhumid regions. Although there are no occurrences of cold-dry MCEs in the warm temperate humid/subhumid region and northern subtropical humid region, cold-dry TCEs frequently occurred in these two regions and with a shorter return period of less than 1 year.

In general, there are 12 CEs types that display broader hotspots and shorter return periods in China from 1961 to 2020: hot-dry (MCEs and TCEs), dry-high fire risk (MCEs and TCEs), high fire risk-strong wind (MCEs and TCEs), hot-dry-high fire risk (MCEs and TCEs), hot-strong wind (TCEs), cold-strong wind (TCEs), hot-dry-strong wind (TCEs), and dry-high fire risk-strong wind (TCEs). Spatially, some humid/subhumid regions of China (including the cold temperate humid region, warm temperate humid/subhumid region, and southern subtropical/tropical humid region) are also hotspots (return period <1 year) of extreme precipitation-strong wind (MCEs and TCEs) and hot-extreme precipitation (TCEs) occurrence. Attention must also be paid to the MCEs of hot-high fire risk and hot-dry-high fire risk-strong wind both in the cold temperature humid region and northern subtropical humid region. In addition, CEs related to cold events also frequently occur in the southern humid regions of China, such as MCEs of hot-high fire risk, cold-strong wind, and cold-dry-strong wind.

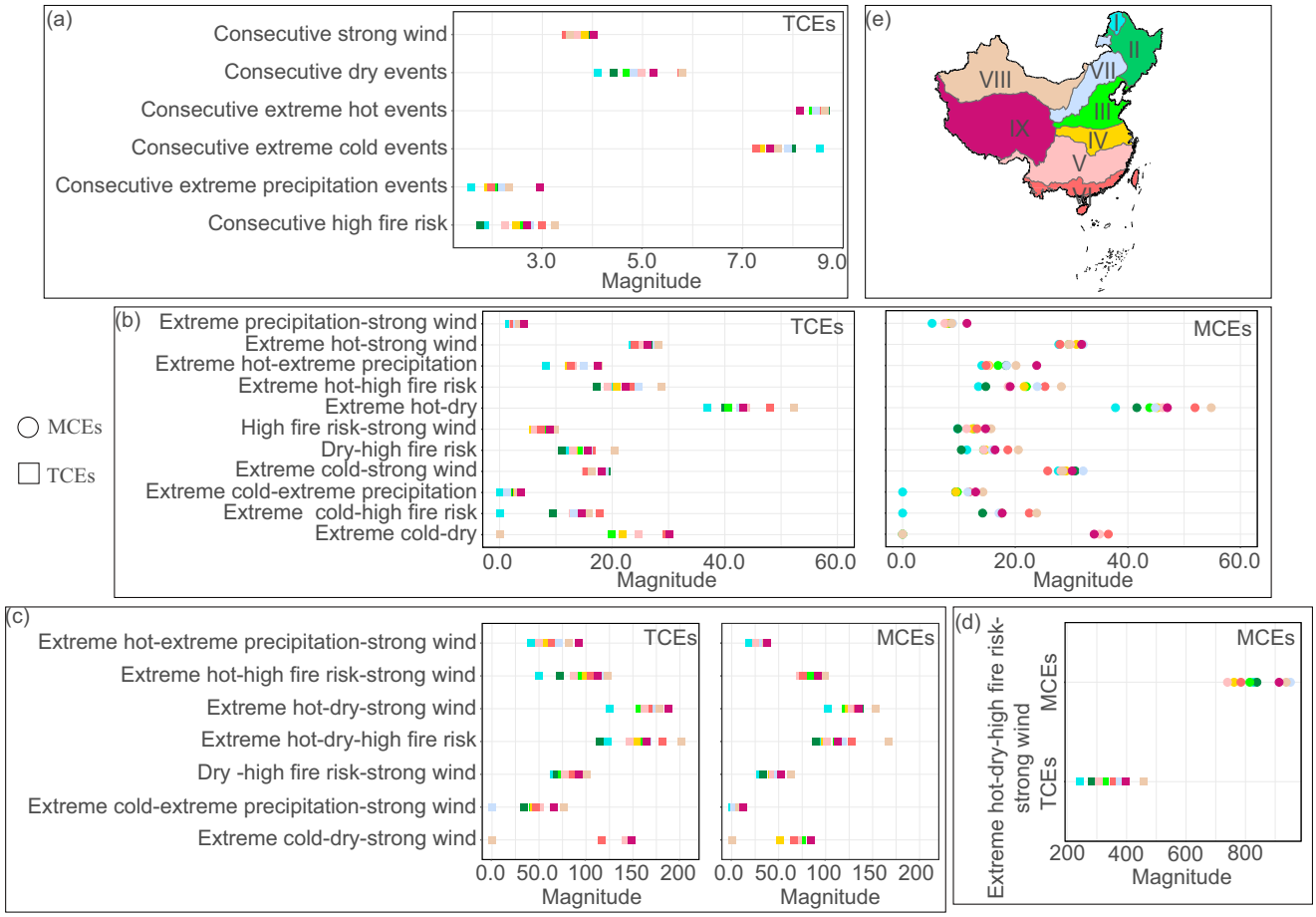


**Fig. 2 The average magnitude of compound events among the nine eco-geographical regions of China from 1961 to 2020. a** is the average magnitude of TCEs formed by one hazard of different eco-geographical regions; (**b**) and (**c**) are the average magnitude of compound events formed by two or three hazard of different eco-geographical regions, respectively; (**d**) is the magnitude of compound extreme hot-dry-high fire risk-strong wind events; (**e**) is the spatial locations of different eco-geographical regions in China.

## Characteristics of MCEs and TCEs

When the number of hazards (two, three, or four) is constant, the average magnitude of CEs related to hot and dry is higher than that of other CEs in the same regions. Among them, the average magnitude of compound hot-dry events is approximately 35 to 52 in China over the past six decades (Fig. 2), which is significantly higher than that of other CEs composed of two hazards in the same region. In contrast, the compound extreme precipitation-strong wind events display the lowest magnitude in the nine regions, with an average magnitude of 5.2 to 11.4. Similarly, the average magnitude of compound hot-dry-strong wind events is also higher than that of other CEs composed of three hazards in the same region, with an average magnitude of 125 to 188.

The combinations (MCEs or TCEs) of various hazards also affect the magnitude of compound events when everything else remains unchanged. Nationally, most MCEs, except for MCEs of hot-high fire risk, cold-dry, and cold-dry-strong wind, display a higher magnitude than those of corresponding TCEs formed by the same hazards. The difference in magnitude between MCEs and TCEs is obvious with an increasing number of hazards. The average magnitude of multivariate compound hot-dry-high fire risk-strong wind events is approximately 739 to 950 throughout China, which is approximately 2.1 to 3.6 times those of corresponding TCEs in the same region.

Most of the CEs that broadly occur in China, including CEs of extreme hot-high fire risk, high fire risk-strong wind, extreme hot-dry-high fire risk, extreme hot-dry-strong wind, and dry-high fire risk-strong wind, have high magnitudes in the south and west and low magnitudes in the north and east on the national scale. In addition, CEs related to extreme precipitation, including CEs of extreme hot-extreme precipitation, cold-extreme precipitation, and cold-extreme precipitation-strong wind, also display higher magnitudes in the mid-subtropical humid region and southern subtropical and tropical humid region than in other regions.

The average duration of CEs also varies significantly on the national scale, which is related to the combinations of events (TCEs or MEs), CEs types, and geographical regions (Fig. 3). When CEs are composed of two hazards, the average duration of the MCEs is longer than that of the corresponding TCEs in the same region. As the major CEs types, the average duration of MCEs of hot-dry, dry-high fire risk, and hot-high fire risk are 3 to 4, 3 to 5, and 2 to 3 days in China, respectively, while the average duration of TCEs of hot-dry, dry-high fire risk, and hot-high fire risk are 2 days. When CEs are composed of three hazards, the multivariate compound hot-dry-high fire risk event still has a longer duration of 3 to 5 days, which is longer than that of the corresponding TCEs. However, the average duration of other MCEs is shorter than that of TCEs in the same region. The temporally compound hot-dry-high fire risk-strong wind events also present a longer duration of 4 to 5 days throughout China, which is longer than those of multivariate compound hot-dry-high fire risk-strong wind events. In addition, among TCEs formed by the same hazard, consecutive cold events have a longer duration of 8 to 12 days, especially in the cold temperate humid region, mid-temperate humid/subhumid region, and northwest arid region.

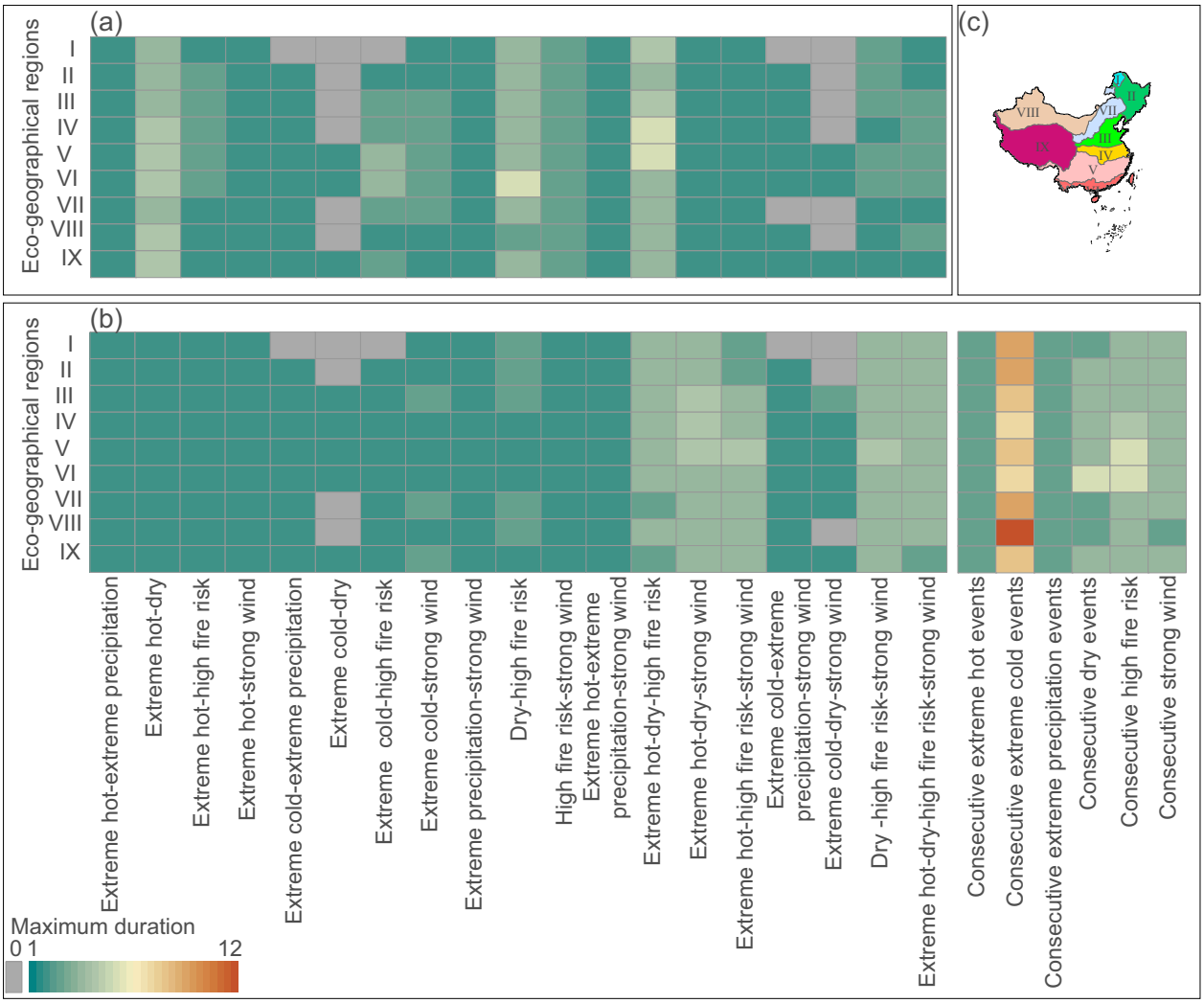


**Fig. 3 The average duration of compound events among the nine eco-geographical regions of China from 1961 to 2020. a**, **b** are the average duration (days) of MCEs and TCEs of different eco-geographical regions over the study period, respectively; (**c**) is the spatial locations of different eco-geographical regions in China.

### Temporal trends in MEs and TCEs from 1961 to 2020

Following the secular trends in features (probability, magnitude, and duration) of compound events from 1961 to 2020, four major trends of CEs are observed (Fig. 4):

(a) Upward trends in probability, magnitude, and duration are observed since 1961. On the national scale, six CEs types exhibit this trend, including consecutive dry events, consecutive high fire risk, hot-dry events (MCEs and TCEs), MCEs of hot-high fire risk and hot-dry-high fire risk. Regionally, the probability, magnitude, and duration of temporal compound hot-high fire risk events also increase in the cold temperate humid region and north semiarid region. In the mid-temperate humid/subhumid region, warm temperate humid/subhumid region, northern subtropical humid region, mid-subtropical humid region, and southern subtropical and tropical humid region, an increasing trend is also detected in some CEs related to extreme precipitation since 1961, including consecutive extreme precipitation events, temporal compound hot-extreme precipitation events, and compound cold-extreme precipitation events (MCEs and TCEs). In general, the above CEs have become more severe and frequent on the national or regional scale over the past six decades.

(b) Increases in probability and decreases in magnitude and duration since 1961. This trend indicated that some CEs are frequent but have low magnitudes or durations in some regions of China. Regionally, the probability of consecutive extreme hot events increase from 1961 to 2020 in China, except for in the cold temperate humid region and southern subtropical and tropical humid region. However, these regions exhibit a decreasing trend in the magnitude or duration of consecutive extreme hot events. Additionally, the northern semiarid region exhibits an increasing trend in probability but a decreasing trend in magnitude or duration of compound hot-extreme precipitation events. Areas with an increasing trend in the probability of CEs of hot-high fire risk and cold-dry are concentrated in the southern subtropical and tropical humid region, but the magnitude and duration of these CEs exhibit decreasing trends in this region since 1961.

(c) Decreases in probability and increases in magnitude and duration are observed since 1961. This trend reveals that some CEs have become intense in certain regions of China from 1961 to 2020. The probability of consecutive extreme precipitation events exhibits a decreasing trend in the cold temperate humid region, mid-temperate humid and subhumid region, warm temperate humid and subhumid

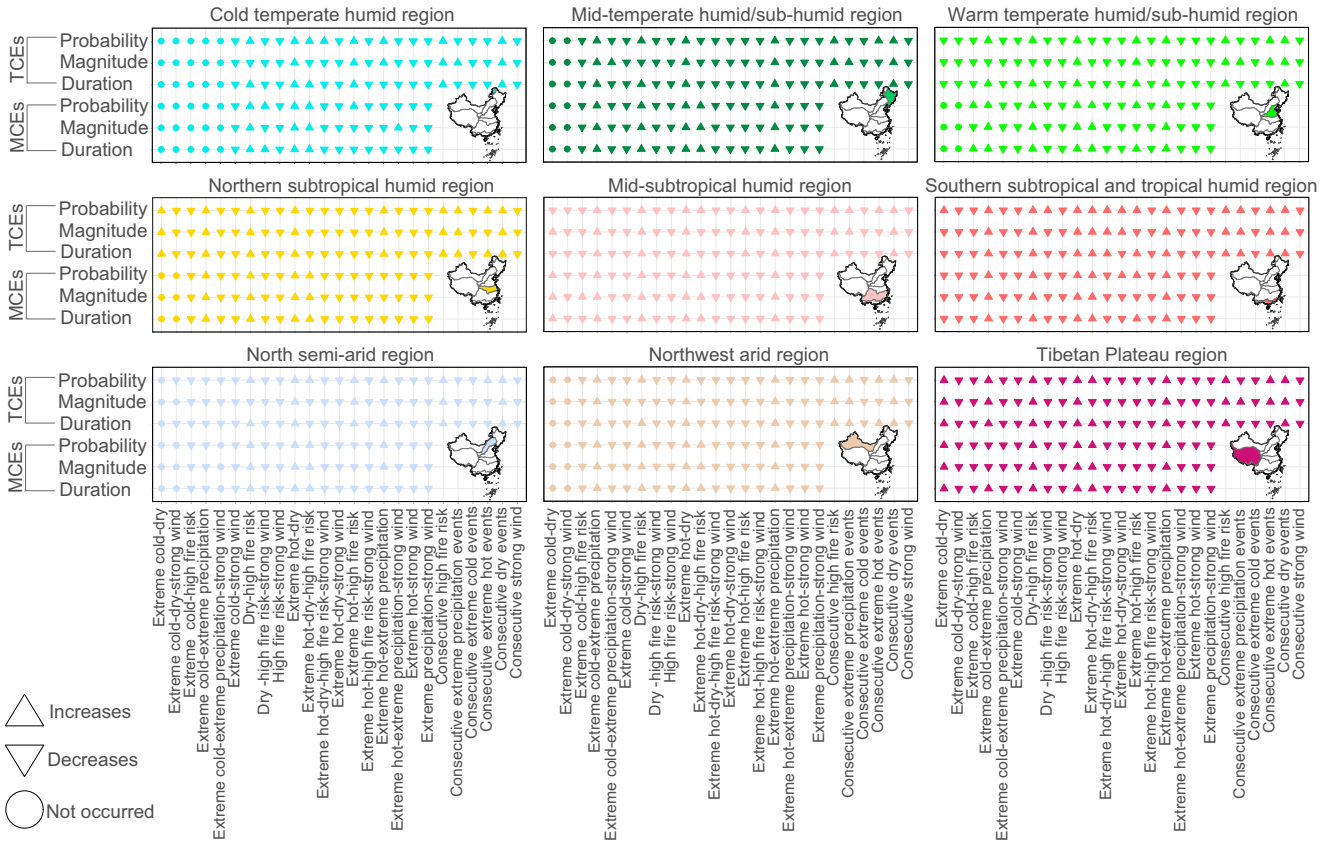


**Fig. 4 Changes in the annual average probability, magnitude, and duration of various compound events in China from 1961 to 2020.** The triangles and inverted triangles represent increasing and decreasing trends, respectively, and circles represent no significant changes.

region, and Tibetan Plateau region, but their magnitude and duration have increased since 1961. In the mid-subtropical humid region, the opposite trend (decreases in probability but increases in magnitude) is observed in the occurrence of temporal compound cold-dry events over the past six decades.

(d) Decreases in probability, magnitude, and duration are observed from 1961 to 2020. On the national scale, the probability, magnitude, and duration of CEs related to strong wind or extreme cold events decreases from 1961 to 2020 (Fig. 4).

### Statistical correlation among various hazards

At the national scale, extreme hot events show a positive correlation with dry events (LMF > 1) and form multivariate compound hot-dry events (Fig. 5). Furthermore, these compound hot-dry events also show a positive correlation with high fire risk and strong wind events (LMF > 1), forming CEs of hot-dry-high fire risk, hot-dry-strong wind, and hot-dry-high fire risk-strong wind. In addition, a positive (LMF > 1) correlation is also detected between dry and high fire risk in China, especially in the cold temperate humid region and mid-subtropical humid region. In contrast, extreme hot events show a negative correlation (LMF < 1) with strong wind events in China.

Areas with a positive correlation (LMF > 1) between extreme hot events and extreme precipitation events are concentrated in the warm temperate humid/subhumid region, northern subtropical humid region, mid-subtropical humid region, and southern subtropical and tropical humid region. These regions also experience temporal compound hot-extreme precipitation events from 1961 to 2020. In most regions, except for the cold temperate humid region and mid-temperate humid/subhumid region, extreme cold events also show a positive correlation (LMF > 1) with extreme precipitation and strong wind events. This phenomenon is more obvious in the mid-subtropical humid region and southern subtropical/tropical humid region.

## DISCUSSION

Studying the occurrence and hotspots of compound events across China is essential for understanding their characteristics, processes, and risks[31]. To enhance the understanding of the occurrence of compound events, we focus on six major hazards and form 44 CEs types in China. From an occurrence time perspective, we find that MCEs and TCEs have similar spatial hotspots and types, but their features (probability, magnitude, and duration) vary on the national and regional scales. On the national scale, multivariate compound hot-dry events show higher probabilities and magnitudes than temporal compound hot-dry events. Previous studies in China focused on temperature-related CEs and found that compound hot-dry events have become more frequent and intense in recent decades at the national scale, possibly due to climate warming and multidecadal/multiannual variability (e.g., El Niño and Pacific Decadal Oscillation)[36–38]. There is a consensus that because of land–atmosphere feedback, extremely hot and dry events are often positively correlated, increasing the probability of compound hot-dry events[40–42]. Our results also indicate that extreme hot events show a positive correlation with dry events in China.

We also note that a positive correlation exists between dry and high fire risk on the national scale. Dry events decrease soil moisture and fuel moisture, which increases the occurrence of high fire risk and causes intense fire behavior[43,44]. Past studies have also shown a strong correlation between drought and high

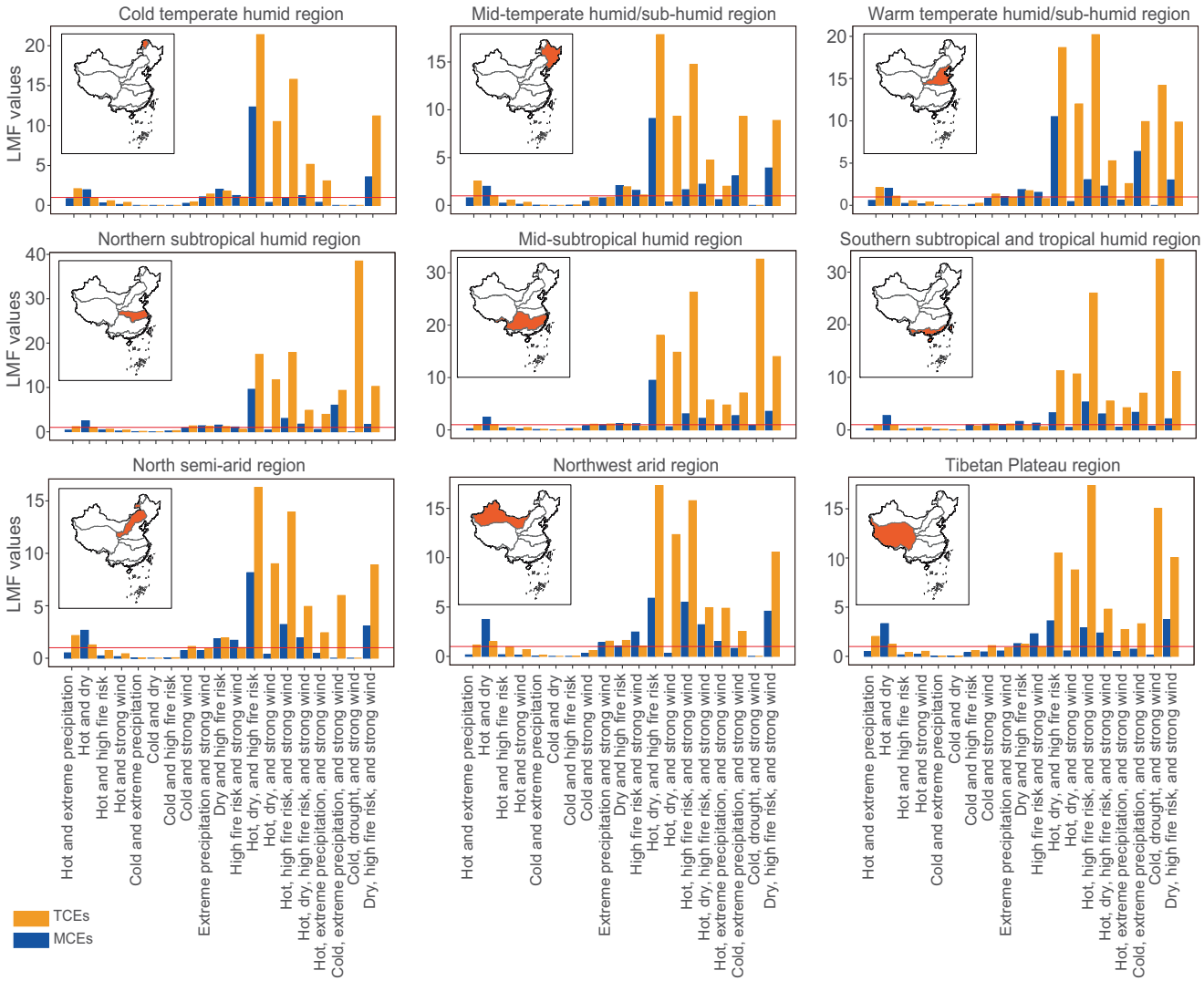


**Fig. 5 LMF values among various hazards in different eco-geographical regions.** The LMF values represent the correlation among various hazards on their joint occurrence probability. The LMF varies between 0 and infinity. If the two hazards are independent, the LMF equals 1. For positively correlated hazard pairs, the LMF is larger than one and increasing with the strength of correlation. For negatively correlated hazards, the LMF falls between 0 and 1.

fire risk by fitting a quantitative relation between drought indices and wildfire numbers or burned areas[45–47]. More importantly, hot and dry conditions enhance evapotranspiration and reduce fuel moisture, leading to an increase in available fuel combustion. Therefore, hot and dry conditions are usually precursors to mega-wildfires[48,49]. Recent extreme events worldwide also showed that the wildfire risk easily reaches an extreme threshold under the influence of compound hot-drought events[50,51]. However, the characteristics and spatiotemporal trends of such compound dry-high fire risk events are still unclear on a larger scale. Since 1961, compound hot-dry-high fire risk events have become more intense and frequent across China. These phenomena indicate that China has experienced an increasing wildfire risk over the past six decades. Furthermore, there is also a positive correlation between high fire risk and strong wind in most regions of China. Such compound high fire risk-strong wind events are also characterized by high probabilities and magnitudes. Strong wind events are conducive to wildfire spread and the formation of larger burned areas[52,53] and increase the possibility of surface fires transforming into crown fires and extreme fire behavior[54,55].

Regionally, temporally compounded extreme hot-extreme precipitation events occur frequently and broadly in humid regions of China over the past decades. An increasing trend is also detected in the frequency of temporal compound hot-extreme precipitation events, especially in the southern humid regions of China[27–29]. The results from the LMF indicate that in humid regions of China, extreme hot events also show a positive correlation with extreme precipitation, forming temporal compound extreme hot-extreme precipitation events. Theoretically, rising air temperature also increases the water-holding capacity of the atmosphere to a certain extent, and such high temperatures and humid conditions may lead to atmospheric instability and convection for precipitable water over a local range[56]. This leads to condensed water and sudden extreme precipitation after the end of a hot event[28,57,58]. In addition, tropical cyclones and strong convective weather systems may induce compound extreme precipitation-strong wind events, especially in coastal areas of southeast China[23]. Our results also reveal such compound events and we find that their probability and magnitude have decreased since 1961, which is consistent with the change in strong wind events[23].

With climate warming, the probability of CEs related to extreme cold events has decreased over the past six decades. The results from past studies also revealed a decreasing trend in the

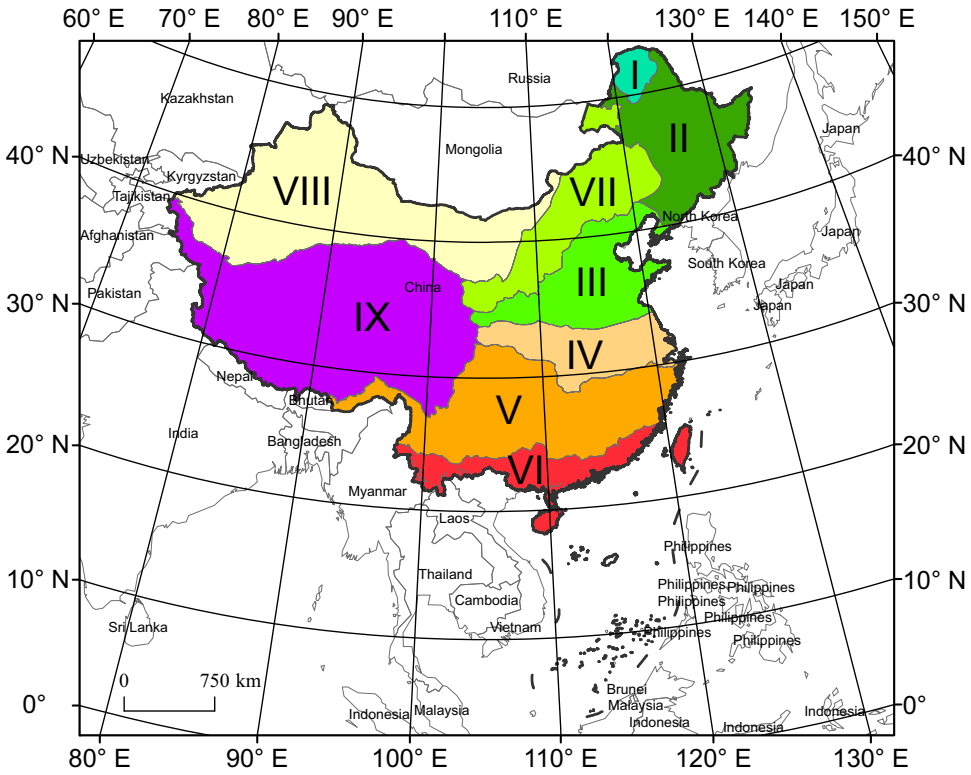


**Fig. 6 Study area and eco-geographical regions.** Where (I) to (IX) are the cold temperate humid region, mid-temperate humid/subhumid region, warm temperate humid/subhumid region, northern subtropical humid region, mid-subtropical humid region, southern subtropical and tropical humid region, north semiarid region, northwest arid region, and Tibetan Plateau region.

frequency of compound dry–wet events in the humid and semihumid monsoon regions of eastern China[59] and the Qinghai-Tibet region[60]. We note that compound cold-extreme precipitation events show a positive correlation with strong wind events, forming compound cold-extreme precipitation-strong wind events in certain parts of eastern China. These compound events are related to anomalous atmospheric circulations (such as the Siberian high and the north polar vortex at high latitudes and La Niña)[61]. In addition, compound cold-high fire risk events that are related to the fire season also occur in the humid regions of South China[62].

In this study, the bottom-up method highlighted by Zscheischler et al. (2018) is used to improve the CE recognition method[19] used in previous studies. The bottom-up method usually starts from a single disaster and identifies all of the disasters that play a role in compound event combinations[9]. Most studies have focused more on hot and drought indices in compound hot-drought events[37,38,63] or ignored strong wind events in flooding analysis[23]. Therefore, these improved methods can enhance the recognition and classification accuracy of multivariate and temporal compound events formed by multiple hazards. On the other hand, in this study, we mainly consider the continuous occurrence of hazards in the identification of TCEs. Theoretically, the combination of different hazards that continuously occur over a short-term period is also considered a TCEs, such as the extreme precipitation events occurring within three days after hot events[28] and two (or more) extreme precipitation days separated by one nonextreme day[64]. However, the temporal threshold is difficult to define due to regional asymmetry. A key premise of using this method is to ensure that the impacts of hazards are cumulative, which is also an important feature of CEs[5]. In contrast, although the framework proposed in this study does not consider a temporal threshold, it can highlight the importance of the cumulative impacts of hazards. We suggest that a temporal threshold can be determined according to the cases of CEs in different regions to enhance the recognition accuracy of TCEs. Due to data limitations, this study mainly explores the spatio-temporal patterns of 44 CEs types on the national scale and ignores other hazards (such as river depletion or pollution). A more comprehensive database of hazards should be compiled in the future to further strengthen the understanding of CEs. In short, this study provides a basic theoretical framework for understanding the occurrence of CEs at the national scale, and the results are helpful for assessing CEs risks and implementing mitigation strategies in the future.

## METHODS

### Data sources

Daily meteorological observations from 1961 to 2020 in mainland China are obtained from the Meteorological Information Center. Daily weather data include the maximum, minimum and average air temperature (°C), precipitation (mm), wind speed (m/s), and relative humidity (%). A total of 2017 stations are screened in this study, with variables missing in less than 5% of the study period at each station. Multiple linear regression analysis is used to interpolate these missing variables[65].

Based on the characteristics of the ecogeographical system (topography, vegetation, and climate), China is divided into nine regions (Fig. 6): the cold temperate humid region (I), mid-temperate humid/subhumid region (II), warm temperate humid/subhumid region (III), northern subtropical humid region (IV), mid-subtropical humid region (V), southern subtropical and tropical humid region (VI), north semiarid region (VII), northwest arid region (VIII), and Tibetan Plateau region (IX)[66].

**Table 1.** Descriptions of the selected extreme event indices and abbreviations in this study.

| Abbreviation | Definition |
|---|---|
| TX90p | Percentage of days when daily maximum temperature is > the 90th percentile for the period from 1961 to 2020 |
| TN10p | Percentage of days when daily minimum temperature is < the 10th percentile for the period from 1961 to 2020 |
| R90th | Percentage of days when daily precipitation is > the 90th percentile for the period from 1961 to 2020 |
| VPD90p | Percentage of days when VPD is > the 90th percentile for the period from 1961 to 2020 |
| FWI90p | Percentage of days when daily FWI is > the 90th percentile for the period from 1961 to 2020 |
| WS90p | Percentage of days when wind speed is > the 90th percentile for the period from 1961 to 2020 |

### Extreme event index calculation and compound event definition

Considering that climate variables show multiple and complex features in different regions, the percentile method is used to identify the threshold for extreme events for each station (Table 1)[23]. Notably, when obtaining the extreme precipitation threshold, we exclude records with daily precipitation amounts of less than 0.1 mm/day at each station.

The vapor pressure deficit (VPD), calculated as the difference between the actual vapor pressure ($e_a$) and the saturation vapor pressure ($e_s$), is used to indicate dry conditions at the daily scale[67]. Recent studies have revealed that although precipitation deficits are a prerequisite for drought occurrence, they cannot be used to detect the relevant changes in increasing drought on a regional or global scale under climate warming[68–70]. These studies paid more attention to the importance of elevated temperature in understanding drought features and utilized VPD to detect short-term drought events[69–71]. Over the past two decades, the annual average VPD has been increasing in China, showing similar spatial trends in dryness and wetness changes with the standardized precipitation evapotranspiration index (SPEI)[72]. Here, we calculate $e_s$ and $e_a$ as follows:

$$e_s = \frac{e^0(T_{max}) + e^0(T_{min})}{2} = \frac{0.6108\exp\left[\frac{17.27T_{min}}{T_{min}+237.3}\right] + 0.6108\exp\left[\frac{17.27T_{max}}{T_{max}+237.3}\right]}{2} \quad (1)$$

$$e_a = e_s \times \frac{RH}{100} \quad (2)$$

where $T_{max}$ and $T_{min}$ are the daily maximum and minimum temperatures (°C), respectively, and $RH$ indicates the average monthly relative humidity.

The daily fire weather index (FWI) is calculated for each station using the 'cffdrs' package in R software based on daily temperature, relative humidity, wind speed, and 24-h precipitation from 1961 to 2020[73]. This index combines the rate of fire spread and the build-up index and represents potential fire intensity. The FWI has a strong positive correlation with burned areas across most of the burnable land masses worldwide and can reflect the fire risk.

The binary variable method is used to identify the occurrence of every hazard, where 1 represents the occurrence of a hazard and 0 represents no occurrence on a given day ($i$). The occurrence of MCEs and TCEs at each station within the past six decades is calculated using Eq. (3) and Eq. (4), respectively. For instance, if a station experiences extreme hot ($X_i^{TX90p} = 1$) and dry ($X_i^{VPD90p} = 1$) conditions on the same day $i$ (from 1 to 365), it is categorized as a multivariate compound hot-dry event. The succession of hazards can be of the same type or consecutive occurrences of different hazards[5]. For example, if an extreme hot event (day $i$) is followed by a dry event (day $i+1$), it is classified as a temporally compound hot-dry event. Daily extreme precipitation events that exceed the threshold for two or more consecutive days are defined as consecutive extreme precipitation events[64].

$$MCEs_i = \begin{cases} 1, & X_i^{TX90p} + X_i^{TN10p} + X_i^{R90th} + X_i^{VPD90p} + X_i^{FWI90p} + X_i^{WS90p} \geq 2 \\ 0, & \text{otherwise} \end{cases} \quad (3)$$

$$TCEs_i = \begin{cases} 1, & \sum_{j=i}^{i+n} X_j^a = n+1 (i+n = 2 \text{ to } 365, a \in \text{six hazards}) \\ 0, & \text{otherwise} \end{cases} \quad (4)$$

### Analyzing the features of compound events

Here, we focus on the four main characteristics of CEs: probability, return period, maximum duration, and magnitude. Specifically, the probability ($P^{ab}$) of a compound event ($CEs^{ab}$) is defined as the ratio of the number of days on which the CEs occur ($\sum_{i=1}^{n} Days(CEs^{ab} = 1)_i$) to the total number of days in the study period ($P^{ab} = \frac{\sum_{i=1}^{n} Days(CEs^{ab}=1)_i}{1961-2020 \text{ periods}}$). Then, the return period (yrs) is calculated from the inverse relationship between the probability and recurrence period ($RP_{ab} = \frac{1}{P_{ab} \times 365}$)[19]. The maximum duration is defined as the longest period (in days) during which a compound event occurs on a monthly or annual scale (Eq. (5)).

$$Duration_{max} = \max\left(length\left\{CEs_i^{ab} \bigcap CEs_{i+1}^{ab} \ldots \bigcap CEs_{i+n}^{ab}\right\}\right) \quad (5)$$

For each station, we normalize the six extreme indices using a modified polar transformation (Eq. (6)) to remove the effects of differences in magnitude.

$$\hat{Y}_i = \begin{cases} (1 - \frac{Y_i - Y_{min}}{Y_{max} - Y_{min}}) \times 10 & Y \in T_{min} \\ (\frac{Y_i - Y_{min}}{Y_{max} - Y_{min}}) \times 10 & Y \in \text{other extreme indices} \end{cases} \quad (6)$$

where $Y_i$ is the value of the extreme indices on day $i$, and $Y_{min}$ and $Y_{max}$ are the maximum and minimum values of the extreme indices for the period from 1961 to 2020, respectively. $\hat{Y}_i$ is the normalized value, which ranges from 0 to 10.

We express the magnitude index (MI) of compound events as an intensity product of normalized extreme indices[23]. The MI can be calculated as follows:

$$MI_i^{ab} = \hat{Y}_i^{\,a} \times \hat{Y}_i^{\,b} \quad (7)$$

where $i$ is the time step (from 1 to 365) at each station and $\hat{Y}_i^{\,a}$ and $\hat{Y}_i^{\,b}$ are the normalized values of hazards $a$ and $b$, respectively.

The Mann–Kendall nonparametric test[74] is utilized to analyze temporal trends in the features of CEs over the past six decades. The statistical value $S$ is calculated using the subsequent

Received: 18 April 2023; Accepted: 27 September 2023;
Published online: 23 October 2023

Xuezheng Zong[1,2], Yunhe Yin[1]✉, Mijia Yin[1,2], Wenjuan Hou[1], Haoyu Deng[1] and Tong Cui[3]✉
[1]Key Laboratory of Land Surface Pattern and Simulation, Institute of Geographic Sciences and Natural Resources Research, Chinese Academy of Sciences, Beijing 100101, China. [2]University of Chinese Academy of Sciences, Beijing 100049, China. [3]National Climate Center, China Meteorological Administration, Beijing 100081, China.
✉email: yinyh@igsnrr.ac.cn; cuitong@cma.gov.cn

equations:

$$Z = \begin{cases} \frac{S+1}{\sqrt{\mathrm{Var}(S)}}, & \text{if} S < 0 \\ 0, & \text{if} S = 0 \\ \frac{S-1}{\sqrt{\mathrm{Var}(S)}}, & \text{if} S > 0 \end{cases} \quad (8)$$

$$S = \sum_{i=1}^{n-1} \sum_{j=i+1}^{n} \sin(c_i - c_j) \quad (9)$$

where $n$ is the number of data points and $c_i$ and $c_j$ are the data values in the time series $i$ and $j$ ($i < j$), respectively. $\sin(c_i - c_j)$ is the characterization function.

$$\sin(x_i - x_j) = \begin{cases} 1, \text{if } c_i - c_j < 0 \\ 0, \text{if } c_i - c_j = 0 \\ -1, \text{if } c_i - c_j > 0 \end{cases} \quad (10)$$

The standard deviation Var($S$) is calculated using the following equation:

$$\mathrm{Var}(S) = \frac{n(n-1)(2n+5) - \sum_{i=1}^{m} t_i(t_i-1)(2t_i+5)}{18} \quad (11)$$

In this study, $z > 0$ represents a consistently increasing trend, while $z < 0$ indicates a decreasing trend. The trends are divided into five classes: significant increase ($z \geq 1.96$), slight increase ($0 < z < 1.96$), no change ($z = 0$), slight decrease ($-1.96 < z < 0$), and significant decrease ($z \leq -1.96$).

### Exploring the correlation among various hazards

We employ the likelihood multiplication factor (LMF) to explore the correlation among various hazards on their joint occurrence probability[19,40,75]. Theoretically, the joint occurrence probability ($P_{\mathrm{indep}}$) of multiple hazards can be expressed as follows if they are independent:

$$P_{\mathrm{indep}} = \frac{\sum_{i=1}^{n} \mathrm{Days}(\mathrm{Events}^{a} = 1)_i}{1961 - 2020 \text{ periods}} \times \frac{\sum_{i=1}^{n} \mathrm{Days}(\mathrm{Events}^{b} = 1)_i}{1961 - 2020 \text{ periods}} \times \ldots \times \frac{\sum_{i=1}^{n} \mathrm{Days}(\mathrm{Events}^{c} = 1)_i}{1961 - 2020 \text{ periods}}$$

However, the actual co-occurrence probability ($P_{\mathrm{actual}}$) is given by:

$$P_{\mathrm{actual}} = \frac{\sum_{i=1}^{n} \mathrm{Days}(\mathrm{CE}^{ab..c} = 1)_i}{1961 - 2020 \text{ periods}} \quad (13)$$

Therefore, the LMF is calculated as the ratio of $P_{\mathrm{actual}}$ to $P_{\mathrm{indep}}$, represented by the following equation:

$$\mathrm{LMF} = \frac{P_{\mathrm{actual}}}{P_{\mathrm{indep}}} = \begin{cases} <1, & \text{negativecorrelation} \\ = 1, & \text{independent} \\ >1, & \text{positivecorrelation} \end{cases} \quad (14)$$

The value of LMF can range from 0 to infinity. In the case where the occurrences of hazards $a$, $b$, and $c$ are independent of each other, the LMF equals 1. A value of LMF < 1 suggests a negative correlation among the occurrences of hazards $a$, $b$, and $c$, while LMF > 1 indicates a positive correlation[19].

## DATA AVAILABILITY

The datasets generated and analyzed during the current study are not publicly available due to intellectual property and patenting process but is available from the corresponding author for academic purposes upon reasonable request.

## CODE AVAILABILITY

Post-processing R scripts for metric computation, bootstrapping, and jitter plots are available from the corresponding author on reasonable request

## REFERENCES

1. Boone, C. D., Bernath, P. F. & Fromm, M. D. Pyrocumulonimbus Stratospheric Plume Injections Measured by the ACE-FTS. *Geophys. Res. Lett.* **47**, e2020GL088442 (2020).
2. Johnston, S. G. & Maher, D. T. Drought, megafires and flood - climate extreme impacts on catchment-scale river water quality on Australia's east coast. *Water Res* **218**, 118510 (2022).
3. Kemter, M. et al. Cascading Hazards in the Aftermath of Australia's 2019/2020 Black Summer Wildfires. *Earth's Future* **9**, e2020EF001884 (2021).
4. Hao, Z. et al. The 2022 Sichuan-Chongqing spatio-temporally compound extremes: a bitter taste of novel hazards. *Science Bulletin* **68**, 1337–1339 (2023).
5. Zscheischler, J. et al. A typology of compound weather and climate events. *Nat. Rev. Earth Env.* **1**, 333–347 (2020).
6. Seneviratne, S.I. et al. Weather and Climate Extreme Events in a Changing Climate. In *Climate Change 2021: The Physical Science Basis. Contribution of Working Group I to the Sixth Assessment Report of the Intergovernmental Panel on Climate Change* 1513–1766, (Cambridge University Press, 2021).
7. Abram, N. J. et al. Connections of climate change and variability to large and extreme forest fires in southeast Australia. *Commun. Earth Environ.* **2**, 8 (2021).
8. Jones, M. W. et al. Global and regional trends and drivers of fire under climate change. *Rev. Geophys.* **60**, e2020RG000726 (2022).
9. Zscheischler, J. et al. Future climate risk from compound events. *Nat. Clim. Change* **8**, 469–477 (2018).
10. Ridder, N. N., Ukkola, A. M., Pitman, A. J. & Perkins-Kirkpatrick, S. E. Increased occurrence of high impact compound events under climate change. *NPJ Clim. Atmos. Sci.* **5**, 3 (2022).
11. AghaKouchak, A., Cheng, L., Mazdiyasni, O. & Farahmand, A. Global warming and changes in risk of concurrent climate extremes: Insights from the 2014 California drought. *Geophys. Res. Lett.* **41**, 8847–8852 (2014).
12. Ribeiro, A. F. S., Russo, A., Gouveia, C. M. & Pires, C. A. L. Drought-related hot summers: A joint probability analysis in the Iberian Peninsula. *Weather Clim. Extreme* **30**, 100279 (2020).
13. Brando, P. M. et al. Abrupt increases in Amazonian tree mortality due to drought–fire interactions. *P. Natl. Acad. Sci. USA* **111**, 6347–6352 (2014).
14. Fairman, T. A., Nitschke, C. R. & Bennett, L. T. Too much, too soon? A review of the effects of increasing wildfire frequency on tree mortality and regeneration in temperate eucalypt forests. *Int. J. Wildland Fire* **25**, 831–848 (2016).
15. Littell, J. S., Peterson, D. L., Riley, K. L., Liu, Y. & Luce, C. H. A review of the relationships between drought and forest fire in the United States. *Global Change Biol* **22**, 2353–2369 (2016).
16. Berghuijs, W. R., Woods, R. A., Hutton, C. J. & Sivapalan, M. Dominant flood generating mechanisms across the United States. *Geophys. Res. Lett.* **43**, 4382–4390 (2016).
17. Berghuijs, W. R., Harrigan, S., Molnar, P., Slater, L. J. & Kirchner, J. W. The Relative Importance of Different Flood-Generating Mechanisms Across Europe. *Water Resour. Res.* **55**, 4582–4593 (2019).
18. Deb, P. et al. Causes of the Widespread 2019–2020 Australian Bushfire Season. *Earth's Future* **8**, e2020EF001671 (2020).
19. Ridder, N. N. et al. Global hotspots for the occurrence of compound events. *Nat. Commun.* **11**, 5956 (2020).
20. Mukherjee, S. & Mishra, A. K. Increase in Compound Drought and Heatwaves in a Warming World. *Geophys. Res. Lett.* **48**, e2020GL090617 (2021).
21. Feng, Y., Liu, W., Sun, F. & Wang, H. Changes of compound hot and dry extremes on different land surface conditions in China during 1957–2018. *Int. J. Climatol.* **41**, E1085–E1099 (2021).
22. Shi, H. et al. Co-occurrence of California Drought and Northeast Pacific Marine Heatwaves Under Climate Change. *Geophys. Res. Lett.* **48**, e2021GL092765 (2021).
23. Zhang, Y., Sun, X. & Chen, C. Characteristics of concurrent precipitation and wind speed extremes in China. *Weather Clim. Extreme* **32**, 100322 (2021).

24. Zhang, S. et al. Revealing the Circulation Pattern Most Conducive to Precipitation Extremes in Henan Province of North China. *Geophys. Res. Lett.* **49**, e2022GL098034 (2022).
25. Emanuel, K. Assessing the present and future probability of Hurricane Harvey's rainfall. *P. Natl. Acad. Sci. USA* **114**, 12681–12684 (2017).
26. Davenport, F. V., Burke, M. & Diffenbaugh, N. S. Contribution of historical precipitation change to US flood damages. *P. Natl. Acad. Sci. USA* **118**, e2017524118 (2021).
27. Wu, S. et al. Increasing Compound Heat and Precipitation Extremes Elevated by Urbanization in South China. *Front. Earth Sc-Switz* **9** (2021).
28. You, J. & Wang, S. Higher Probability of Occurrence of Hotter and Shorter Heat Waves Followed by Heavy Rainfall. *Geophys. Res. Lett.* **48**, e2021GL094831 (2021).
29. Ning, G. et al. Rising risks of compound extreme heat-precipitation events in China. *Int. J. Climatol.* **42**, 5785–5795 (2022).
30. Chen, D., Norris, J., Thackeray, C. & Hall, A. Increasing precipitation whiplash in climate change hotspots. *Environ. Res. Lett.* **17**, 124011 (2022).
31. Hao, Z. Compound events and associated impacts in China. *iScience* **25**, 104689 (2022).
32. China Meteorological Administration. Blue Book on Climate Change of China 2023. SCIENCE PRESS, Beijing, China. (2023).
33. Chen, Y. & Zhai, P. Revisiting summertime hot extremes in China during 1961–2015: Overlooked compound extremes and significant changes. *Geophys. Res. Lett.* **44**, 5096–5103 (2017).
34. Wang, J. et al. Anthropogenic emissions and urbanization increase risk of compound hot extremes in cities. *Nat. Clim. Change* **11**, 1084–1089 (2021).
35. Wang, J., Feng, J., Yan, Z. & Chen, Y. Future Risks of Unprecedented Compound Heat Waves Over Three Vast Urban Agglomerations in China. *Earth's Future* **8**, e2020EF001716 (2020).
36. Wu, X. et al. Influence of Large-Scale Circulation Patterns on Compound Dry and Hot Events in China. *J. Geophys. Res-Atmos* **126**, e2020JD033918 (2021).
37. Li, H., He, S., Gao, Y., Chen, H. & Wang, H. North Atlantic Modulation of Interdecadal Variations in Hot Drought Events over Northeastern China. *J. Climate* **33**, 4315–4332 (2020).
38. Yu, R. & Zhai, P. More frequent and widespread persistent compound drought and heat event observed in China. *Sci. Rep.* **10**, 14576 (2020).
39. Leonard, M. et al. A compound event framework for understanding extreme impacts. *WIREs Clim. Change* **5**, 113–128 (2014).
40. Zscheischler, J. & Seneviratne, S. I. Dependence of drivers affects risks associated with compound events. *Sci. Adv.* **3**, e1700263 (2017).
41. Yu, H. et al. Hotspots, co-occurrence, and shifts of compound and cascading extreme climate events in Eurasian drylands. *Environ. Int.* **169**, 107509 (2022).
42. Seneviratne, S. I. et al. Investigating soil moisture–climate interactions in a changing climate: A review. *Earth-Sci. Rev.* **99**, 125–161 (2010).
43. Forkel, M. et al. Extreme fire events are related to previous-year surface moisture conditions in permafrost-underlain larch forests of Siberia. *Environ. Res. Lett.* **7**, 044021 (2012).
44. Bastos, A., Gouveia, C. M., Trigo, R. M. & Running, S. W. Analysing the spatio-temporal impacts of the 2003 and 2010 extreme heatwaves on plant productivity in Europe. *Biogeosciences* **11**, 3421–3435 (2014).
45. Zhao, F. & Liu, Y. Important meteorological predictors for long-range wildfires in China. *Forest Ecol. Manag.* **499**, 119638 (2021).
46. Ying, L. et al. Relative humidity and agricultural activities dominate wildfire ignitions in Yunnan, Southwest China: Patterns, thresholds, and implications. *Agr. Forest Meteorol.* **307**, 108540 (2021).
47. Wang, W., Zhao, F., Wang, Y., Huang, X. & Ye, J. Seasonal differences in the spatial patterns of wildfire drivers and susceptibility in the southwest mountains of China. *Sci. Total Environ.* **869**, 161782 (2023).
48. Wang, X., Swystun, T., Oliver, J. & Flannigan, M. D. One extreme fire weather event determines the extent and frequency of wildland fires. *Environ. Res. Lett.* **16**, 114031 (2021).
49. Thompson, D. K., Simpson, B. N., Whitman, E., Barber, Q. E. & Parisien, M.-A. Peatland Hydrological Dynamics as A Driver of Landscape Connectivity and Fire Activity in the Boreal Plain of Canada. *Forests* **10**, 534 (2019).
50. Squire, D. T. et al. Likelihood of unprecedented drought and fire weather during Australia's 2019 megafires. *NPJ Clim. Atmos. Sci.* **4**, 64 (2021).
51. White, R. H. et al. The unprecedented Pacific Northwest heatwave of June 2021. *Nat. Commun.* **14**, 727 (2023).
52. Coen, J. L. & Schroeder, W. The High Park fire: Coupled weather-wildland fire model simulation of a windstorm-driven wildfire in Colorado's Front Range. *J. Geophys. Res-Atmos* **120**, 131–146 (2015).
53. Butler, B. et al. Exploring fire response to high wind speeds: fire rate of spread, energy release and flame residence time from fires burned in pine needle beds under winds up to 27 m $s^{-1}$. *Int. J. Wildland Fire* **29**, 81–92 (2020).
54. Morvan, D. A numerical study of flame geometry and potential for crown fire initiation for a wildfire propagating through shrub fuel. *Int. J. Wildland Fire* **16**, 511–518 (2007).
55. Tachajapong, W., Lozano, J., Mahalingam, S. & Weise, D. R. Experimental modelling of crown fire initiation in open and closed shrubland systems. *Int. J. Wildland Fire* **23**, 451–462 (2014).
56. Berg, P., Moseley, C. & Haerter, J. O. Strong increase in convective precipitation in response to higher temperatures. *Nat. Geosci.* **6**, 181–185 (2013).
57. Molnar, P., Fatichi, S., Gaál, L., Szolgay, J. & Burlando, P. Storm type effects on super Clausius–Clapeyron scaling of intense rainstorm properties with air temperature. *Hydrol. Earth Syst. Sci.* **19**, 1753–1766 (2015).
58. Wang, G. et al. The peak structure and future changes of the relationships between extreme precipitation and temperature. *Nat. Clim. Change* **7**, 268–274 (2017).
59. Zhang, Y., Yang, X. & Chen, C. Substantial decrease in concurrent meteorological droughts and consecutive cold events in Huai River Basin, China. *Int. J. Climatol.* **41**, 6065–6083 (2021).
60. Wu, X., Hao, Z., Hao, F. & Zhang, X. Variations of compound precipitation and temperature extremes in China during 1961–2014. *Sci. Total Environ.* **663**, 731–737 (2019).
61. Hao, Z., Zheng, J., Ge, Q. & Wang, W. C. Historical analogues of the 2008 extreme snow event over Central and Southern China. *Clim. Res.* **50**, 161–170 (2011).
62. Zong, X., Tian, X. & Liu, J. A Fire Regime Zoning System for China. *Front. Forests Global Change.* **4** (2021).
63. Wu, X. et al. Population exposure to compound dry and hot events in China under 1.5 and 2°C global warming. *Int. J. Climatol.* **41**, 5766–5775 (2021).
64. Du, H. et al. Extreme Precipitation on Consecutive Days Occurs More Often in a Warming Climate. *B. Am. Meteorol. Soc* **103**, E1130–E1145 (2022).
65. Tsinko, Y., Bakhshaii, A., Johnson, E. A. & Martin, Y. E. Comparisons of fire weather indices using Canadian raw and homogenized weather data. *Agr. Forest Meteorol.* **262**, 110–119 (2018).
66. Zheng, D. A Study on the Eco-geographic Regional System of China, FAO FRA2000 Global Ecological Zoning Workshop, Cambridge, UK, July, 28–30, 12 (1999).
67. Williams, A. P. et al. Observed Impacts of Anthropogenic Climate Change on Wildfire in California. *Earth's Future* **7**, 892–910 (2019).
68. Gamelin, B. L. et al. Projected U.S. drought extremes through the twenty-first century with vapor pressure deficit. *Sci. Rep.* **12**, 8615 (2022).
69. Diffenbaugh, N. S., Swain, D. L. & Touma, D. Anthropogenic warming has increased drought risk in California. *P. Natl. Acad. Sci. USA* **112**, 3931–3936 (2015).
70. Vicente-Serrano, S. M. et al. Global drought trends and future projections. *Philos. T. R. Soc. A* **380**, 20210285 (2022).
71. Yuan, X. et al. Anthropogenic shift towards higher risk of flash drought over China. *Nat. Commun.* **10**, 4661 (2019).
72. Wu, X. et al. The Effect of Drought on Vegetation Gross Primary Productivity under Different Vegetation Types across China from 2001 to 2020. *Remote Sensing* **14**, 4658 (2022).
73. Wang, X. et al. cffdrs: an R package for the Canadian Forest Fire Danger Rating System. *Ecol. Process.* **6**, 5 (2017).
74. Mann, H. B. Nonparametric Tests Against Trend. *Econometrica* **13**, 245–259 (1945).
75. Zhou, S. et al. Land–atmosphere feedbacks exacerbate concurrent soil drought and atmospheric aridity. *P. Natl. Acad. Sci. USA* **116**, 18848–18853 (2019).

## ACKNOWLEDGEMENTS

This study received financial support from National Natural Science Foundation of China (42377460), the Key Program of National Natural Science Foundation of China (41831174), and the Second Tibetan Plateau Scientific Expedition and Research Program (2019QZKK0403) supported this study.

## AUTHOR CONTRIBUTIONS

X.Z.: Conceptualization, methodology, investigation, writing – original draft and revised. Y.Y.: conceptualization, methodology, investigation, resources, supervision, writing –review. M.Y.: methodology, investigation, writing–revised. W.H.: data collection, methodology, writing –revised. H.D.: data collection, methodology, writing–revised. T.C.: data collection, methodology, investigation, writing –revised.

## COMPETING INTERESTS

The authors declare no competing interests.

## ADDITIONAL INFORMATION

**Supplementary information** The online version contains supplementary material available at https://doi.org/10.1038/s41612-023-00491-3.